

Supplemental Materials

Mitochondrial lineage assignment

To ensure the selection experiment did not confound selection between mitochondrial lineages, which are potentially cryptic species, and selection within a lineage, we determined the major and minor mitochondrial haplotypes present in our samples. This analysis follows previous COI work conducted in *A. tonsa* (1, 2), particularly Figueroa et al. (3). We used a reference COI from Figueroa et al. to align and pull out the COI region in our raw FASTQ files. Variants were called using Varscan2 (4) in the same manner as our full dataset. Because these are pooled data, we cannot determine haplotypes of individuals. Further, if two lineages were present at equal frequencies, it would be difficult to determine which two haplotypes were present; the variants of each would be mixed in these pooled data. We assessed the distribution of allele frequencies to predict the number and frequency of mitochondrial haplotypes present in these data. Given the bimodal distribution of variants, where SNPs are either nearly fixed or absent (Fig. S9), there are likely two mitochondrial lineages present in these samples; one at very high frequency, and the other at low frequency. Looking at the shift in variant frequency from F0 to F25, it is apparent that the low frequency variant drops out over time while the high frequency variant (which is nearly fixed) remains. Because of the low number of variant sites, the high frequency variant also appears to match the reference sequence, which is from an individual from clade X. All results below hold when a reference from a different clade is used instead.

We reconstruct the major and minor haplotypes present in our data. Given the bimodal distribution of variants, we can reconstruct the consensus sequence of the major haplotypes as variants that are nearly fixed, while the minor haplotype consists of the low frequency variants. We only construct the minor haplotypes for F0 samples, as these haplotypes are no longer present by F25. Variants were filtered in R and VCF files containing either the major or minor variants were created. *bcftools* was used to generate consensus sequences for each sample and haplotype and sequences were concatenated with fasta sequences from Figueroa et al. to allow for direct comparisons downstream. This fasta file was aligned with MUSCLE (5), converted to NEXUS format in R using APE (6), and a phylogenetic tree was built using MrBayes (7) using the substitution model HKY + I + G, following Figueroa et al. The plot was generated with ggplot in R (8). The resulting tree clearly shows that the major haplotype is clade X, with a low frequency of clade S present at F0 (Fig. S10). The S clade drops out by F3 and is not present in any samples at F25, including the ambient selection line. Given the low

frequency of clade S and its absence from all lines by F25, the divergence detected in our experiment is not simply due to selection for a mitochondrial clade, but due to selection within individuals of clade X.

Analysis of covariance in allele frequency change

The replicated nature of our experiment coupled with the multiple selection regimes allows us to disentangle the relative contributions of drift and selection on the genome-wide changes in allele frequencies. We use and expand upon the approach developed by Buffalo and Coop (9). This method quantifies genome-wide covariance in the change in allele frequencies between replicates of a single treatment and between treatments to determine the relative contributions of drift and selection as well as to assess the degree of shared selection between selection regimes. Finally, we can leverage the presence of the control ambient line to estimate and remove the effects of the aforementioned estimates of lab adaptation.

First, it is possible to partition the changes in allele frequencies within a treatment into selection and drift components for replicate A as:

$$\Delta P_{t,A} = \Delta_D P_t + \Delta_S P_t$$

where $\Delta_S P_t$ is the change due to selection and $\Delta_D P_t$ is drift. The proportion of change due to selection can be further defined as the allele frequency change due to lab selection common to all replicates within a treatment group, $\Delta_L P_t$, as well as the change due to selection within a specific selection regime, $\Delta_R P_t$. The change in allele frequency in replicate A can be partitioned into,

$$\Delta P_{t,A} = \Delta_D P_t + \Delta_L P_t + \Delta_R P_t$$

Because the terms above are uncorrelated, the variance is,

$$\text{Var}(\Delta p_t) = \text{Var}(\Delta_D P_t) + \text{Var}(\Delta_L P_t) + \text{Var}(\Delta_R P_t)$$

We estimate the shared effects of selection regime from the allele frequency changes as the covariance of allele frequency change between any two replicates,

$$\text{Var}(\Delta_R P_t) = \text{Cov}(\Delta P_{t,A}, \Delta P_{t,B})$$

Where A and B indicate different replicates within a selection regime. Thus, to estimate the total shared response to selection within a selection regime, we estimate the covariance between all pairwise replicates and take their mean. Further, because of the presence of an ambient control line in our study, we can estimate the contribution of adaptation to the lab environment to the overall changes in allele frequency. The shared variance between a selection regime and the control represents the contribution of lab adaptation within a treatment group, again estimated as the mean of all pairwise comparisons between the two groups, giving $\text{Var}(\Delta_L P_t)$. We can subtract this value from the shared response within a selection regime, $\text{Var}(\Delta_R P_t)$, to get an estimate of the response to selection that is independent of estimated average lab selection effect.

After determining the contributions from selective regime and lab adaptation, the remaining variance can be attributed to the drift component. Finally, these values can be divided by the total variance to find the proportion each contributes to the overall variance in change in allele frequency.

Next, we can use similar principles to determine the shared response to selection between each selective regime. Here, the shared response to selection is again the covariance in allele frequency change between any two replicates, as above, but now from two different treatments,

$$\text{Var}(\Delta_R P_t) = \text{Cov}(\Delta p_{t,A}, \Delta p_{t,B})$$

We take the mean of all possible pairwise comparisons between treatments and scale this by the total variance to determine the proportion of total variance of allele frequency change that is shared. Finally, lab adaptation can be estimated and accounted for as described above.

Accounting for shared variance due to limited F0 replication

In these data, covariances are calculated from the change in allele frequency from the same set of F0 samples for all treatments. While these F0 samples likely represent the pre-selective state of the population, replicating these samples in this way leads to a spurious increase in the covariance estimates between samples in different treatments due to shared sampling variance. This is made clear in the covariance heatmap (Fig. S3A) where along the diagonal where the same replicate is compared between treatments the covariance is increased; Fig. S3B shows these covariance calculations in a different format where the same pattern is evident. Similarly, we see the same pattern when the convergence correlation is calculated (Fig. S4). To avoid this inflation, we dropped any covariances between samples with the same F0 reference when calculating shared response to selection. For example, the covariance in allele frequency change between OWA replicate 1 and Acidification replicate 1 would not be included when quantifying the shared selection response between these treatments. While this reduces our replication to an extent, the estimates are likely much more accurate estimates of the true impact of selection on allele frequency changes as all covariances are independent as a result.

Supplemental table 1: Number of loci assigned to each functional category for each SNP set. The first value is the total number of loci, the 2nd is the proportion of the total. P-values from chi-squared tests relative to the genome-wide distribution. Underlined values are significant (Bonferroni correction: $P < 0.05/15 = 0.0033$). The “No Annotation” category refers to loci that were not on a scaffold with any annotated genes, indicating they are likely in fragmented regions of the genome assembly.

	All loci	OWA candidates	Warming candidates	Acidification candidates	Ambient candidates
No annotation	54,228 0.137	<u>702</u> <u>0.089 (p << 0.001)</u>	<u>577</u> <u>0.092 (p < 0.001)</u>	278 0.162 (p = 0.01)	431 0.134 (p=0.94)
Downstream	28,197 0.071	536 0.068 (p = 0.2)	465 0.074 (p = 0.41)	249 0.11 (p < 0.001)	<u>276</u> <u>0.088 (p=0.001)</u>
Exon	229,898 0.583	<u>5,198</u> <u>0.656 (p < 0.001)</u>	<u>4,049</u> <u>0.646 (p < 0.001)</u>	885 0.517 (p = 0.0038)	1,778 0.564 (p=0.29)
Intron	46,837 0.117	<u>809</u> <u>0.102 (p < 0.001)</u>	<u>635</u> <u>0.101 (p < 0.001)</u>	396 0.108 (p = 0.24)	350 0.11 (p=0.24)
Promoter	35,507 0.0899	681 0.086 (p = 0.2)	544 0.087 (p = 0.42)	311 0.107 (p = 0.02)	315 0.10 (p=0.07)

Supplemental table 2: find at the end of this document.

Supplemental Figures

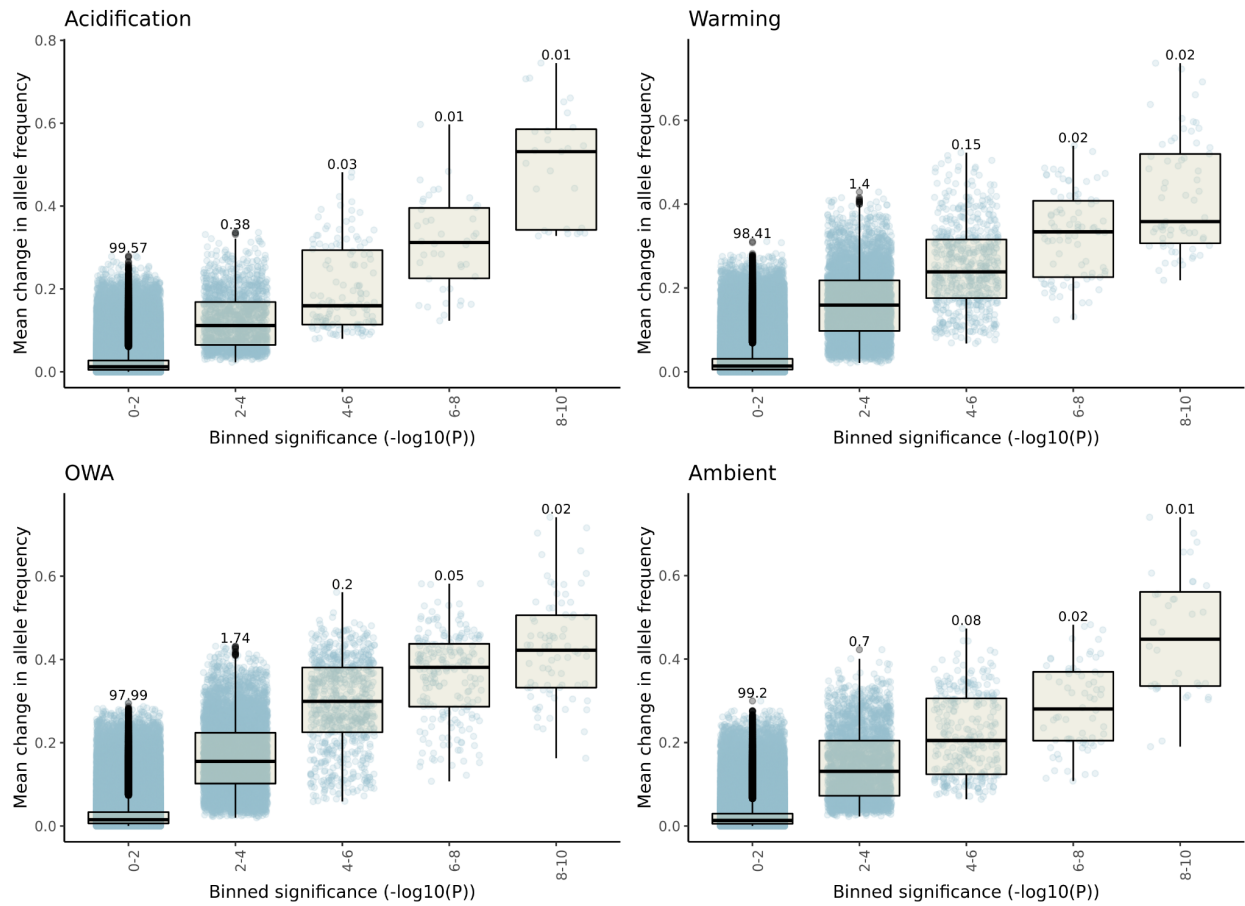


Figure S1: Empirical p-values from drift simulations. Points are individual loci with Tukey's boxplots.
Values above each boxplot indicate the proportion of total loci in that bin.

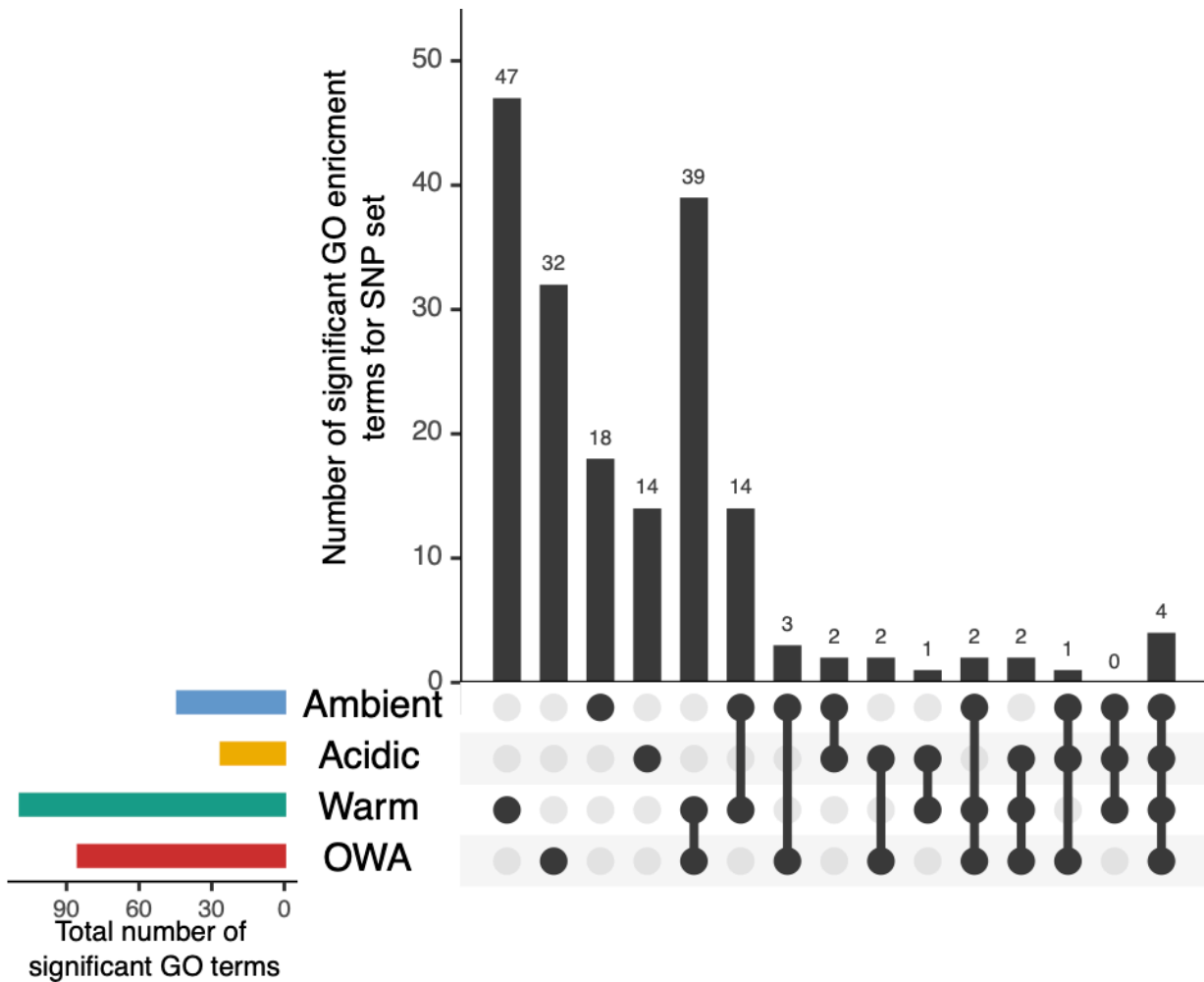


Figure S2. Number of significant go terms per category. Conducted with the same snps as the similar plot in the main text (Fig. 2).

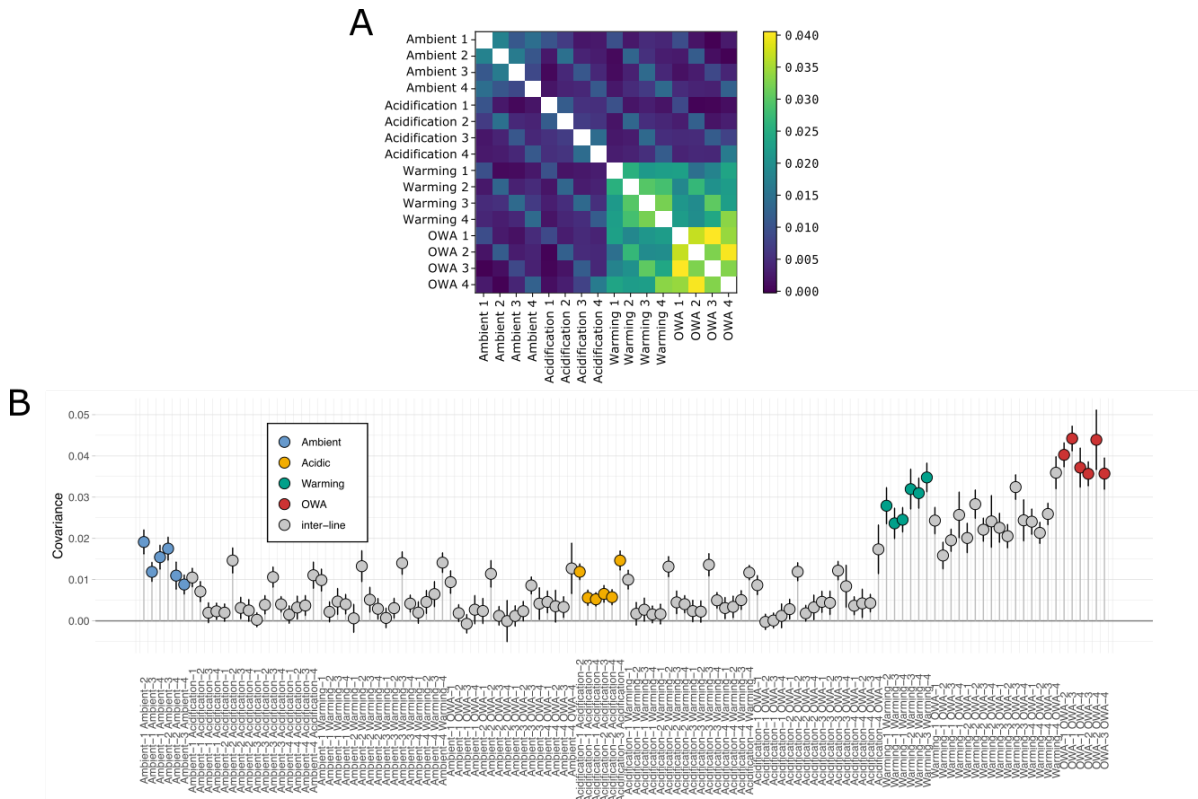


Figure S3: Pairwise covariance in allele frequency change between samples from F0 to F25. A) Each square and color indicate the covariance between two samples. Above the diagonal is a mirror of below. B) The same covariance estimates as in A, but with 95% bootstrap confidence intervals. Color indicates the group comparison. Note the increase in covariance between samples sharing the same replicate number due to an artifact from calculating allele frequency change from the same F0 sample. Samples with shared F0 samples (i.e., the same replicate number) were dropped from further calculations to avoid this bias.

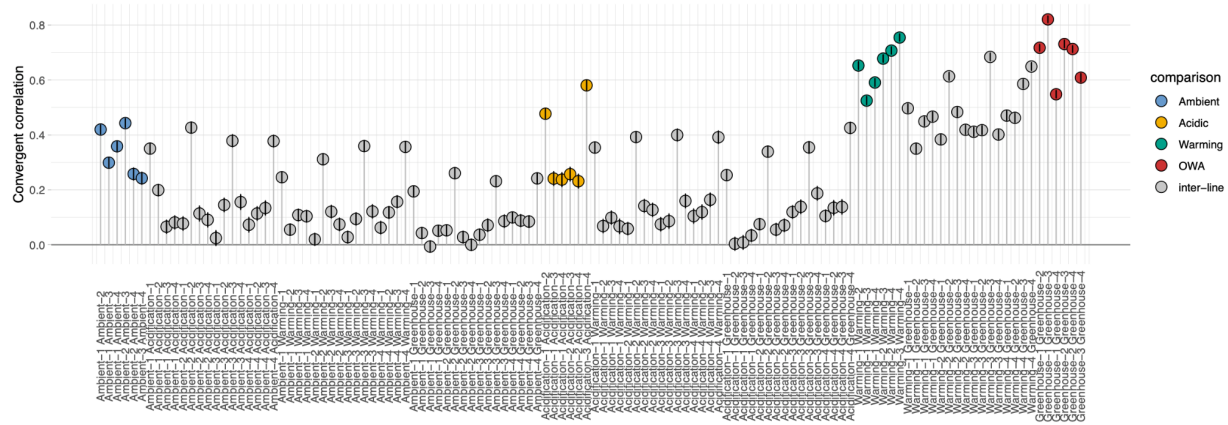


Figure S4: Convergent correlations of allele frequency change from F0 to F25 between samples. Black lines for each point show the 95% bootstrap confidence interval. Note the increase in convergent correlation between samples sharing the same replicate number due to an artifact from calculating allele frequency change from the same F0 sample. Samples with shared F0 samples (i.e., the same replicate number) were dropped from further calculations.

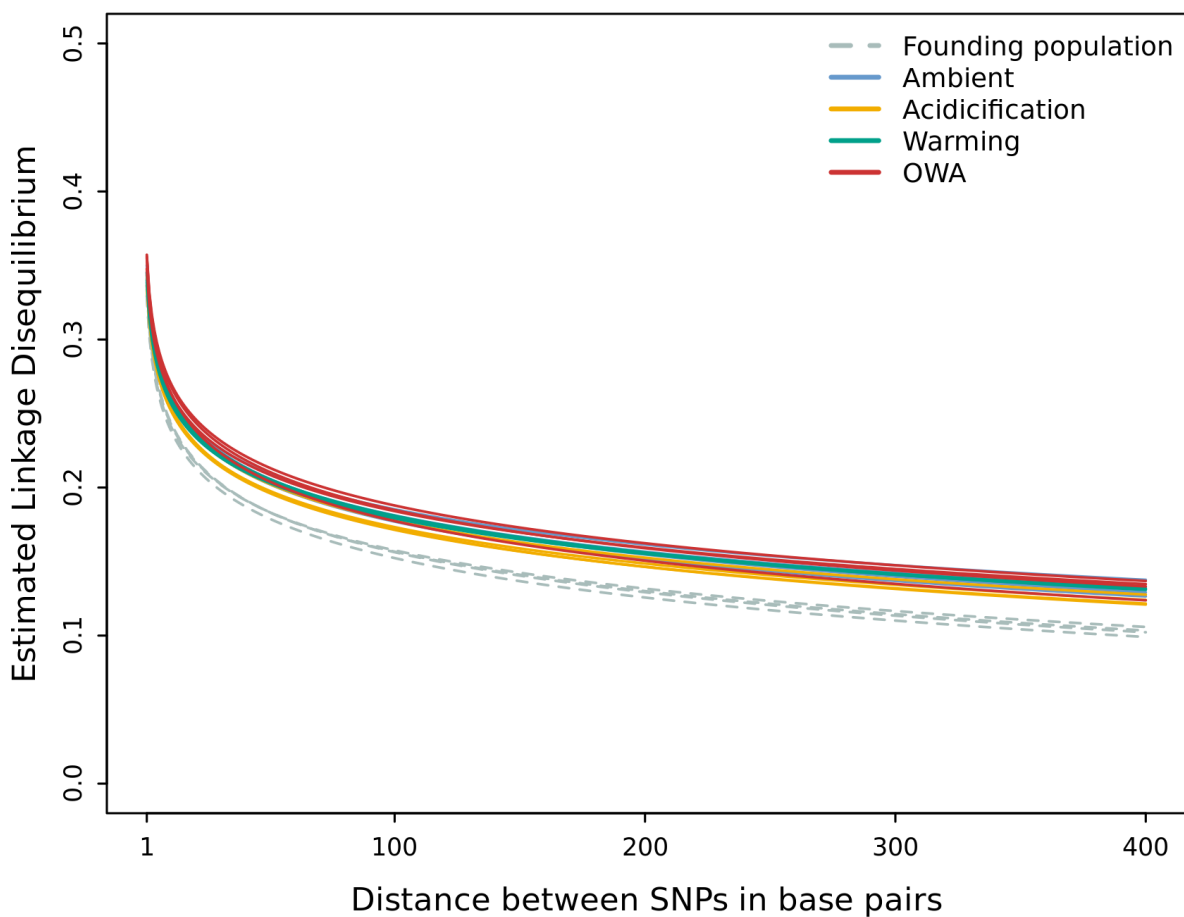


Figure S5: Linkage disequilibrium estimates. Decay curves were fit by regressing the log of the physical distance with LD between base pairs. LD estimates increased with the strength of selection relative to the F0 founding population ($P < 0.001$). Founding population: intercept = 0.212 ± 0.001 , slope = -0.0497 ± 0.0003 ; Ambient: 0.245 ± 0.002 , -0.0562 ± 0.0003 ; Acidification: 0.235 ± 0.001 , -0.0549 ± 0.0003 ; Warming: 0.242 ± 0.001 , -0.0556 ± 0.0003 ; OWA: 0.251 ± 0.002 , -0.058 ± 0.0003

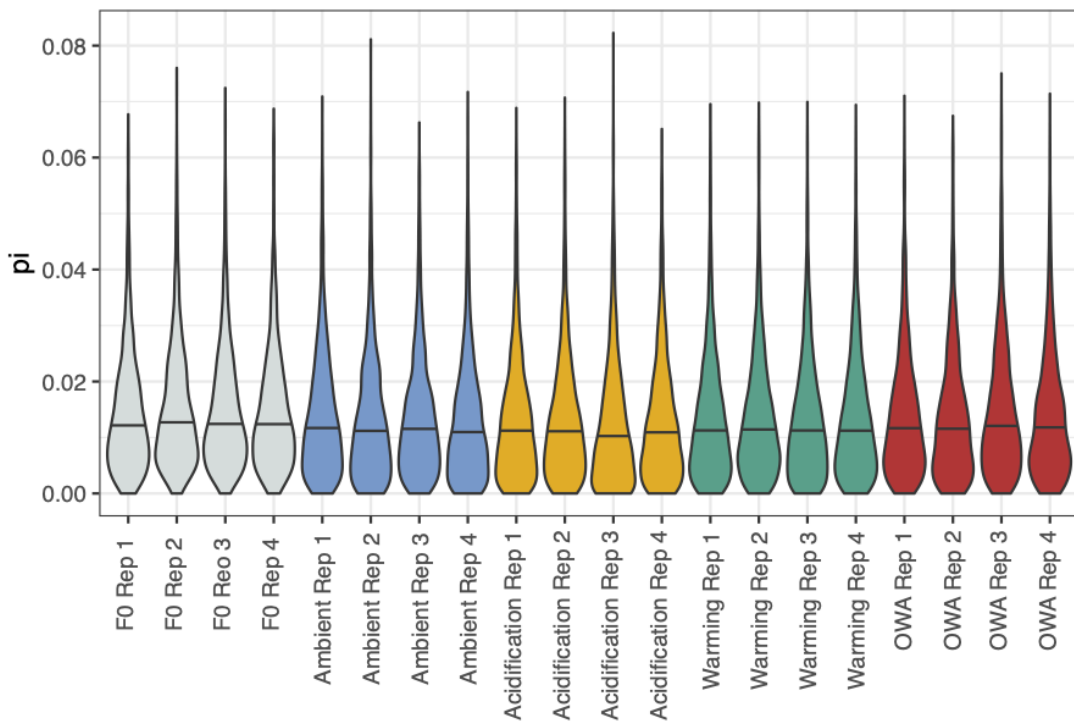


Fig. S6: Genetic diversity estimates. All treatment groups lost genetic diversity relative to the founding F0 population (Wilcoxon signed-rank test, $P < 0.0001$). Estimates for each group: F0 founding population: 0.0148 ± 0.0111 ; ambient: 0.0133 ± 0.0111 ; acidification: 0.0127 ± 0.0111 ; warming: 0.0133 ± 0.0110 ; OWA: 0.0138 ± 0.0112 . Between the F25 treatments, only acidification lines were significantly lower than other lines ($P < 0.001$).

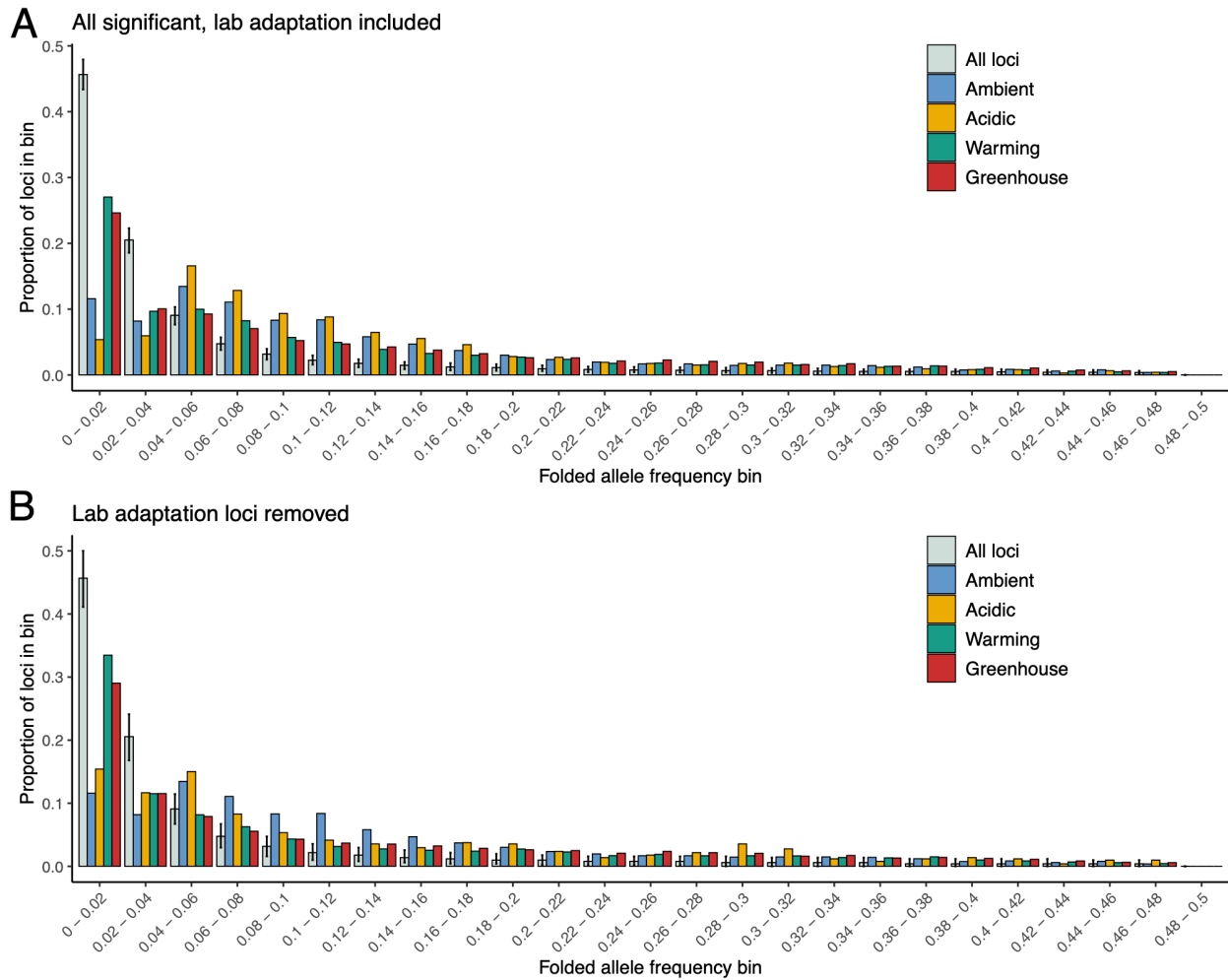


Fig. S7: Starting minor allele frequencies at F0 for loci significant for different treatments. Panel A includes lab adaptation loci in each group while these are removed in panel B. Error bars around the all loci group are 95% confidence intervals from 1000 random samples from all loci where the number of loci sampled was equal to the number of significant Acidification loci (A: 1,713, B: 506). Because the acidification group had the least number of significant loci, these confidence intervals are broader than if sampling was based on warming or OWA values.

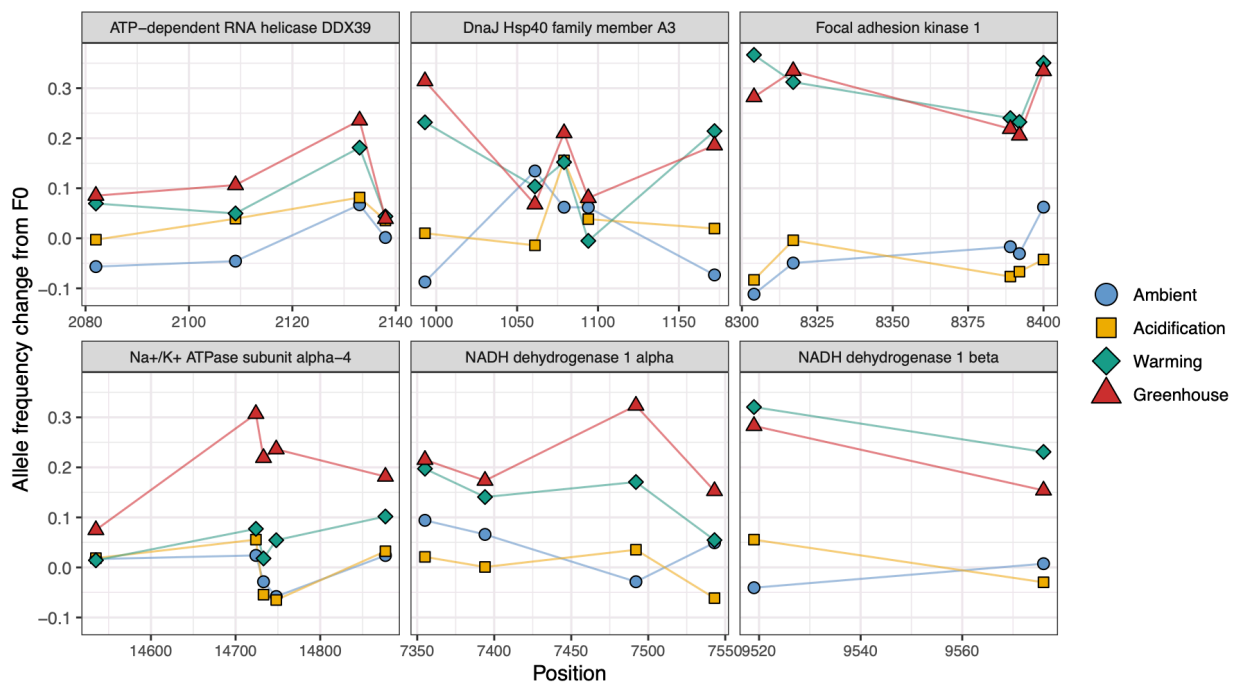


Figure S8: Representative candidate genes underlying rapid adaptation. Points represent the average allele frequency change among replicates from the starting frequencies at F0. Loci have been filtered for minor allele frequency > 0.1 at F0.

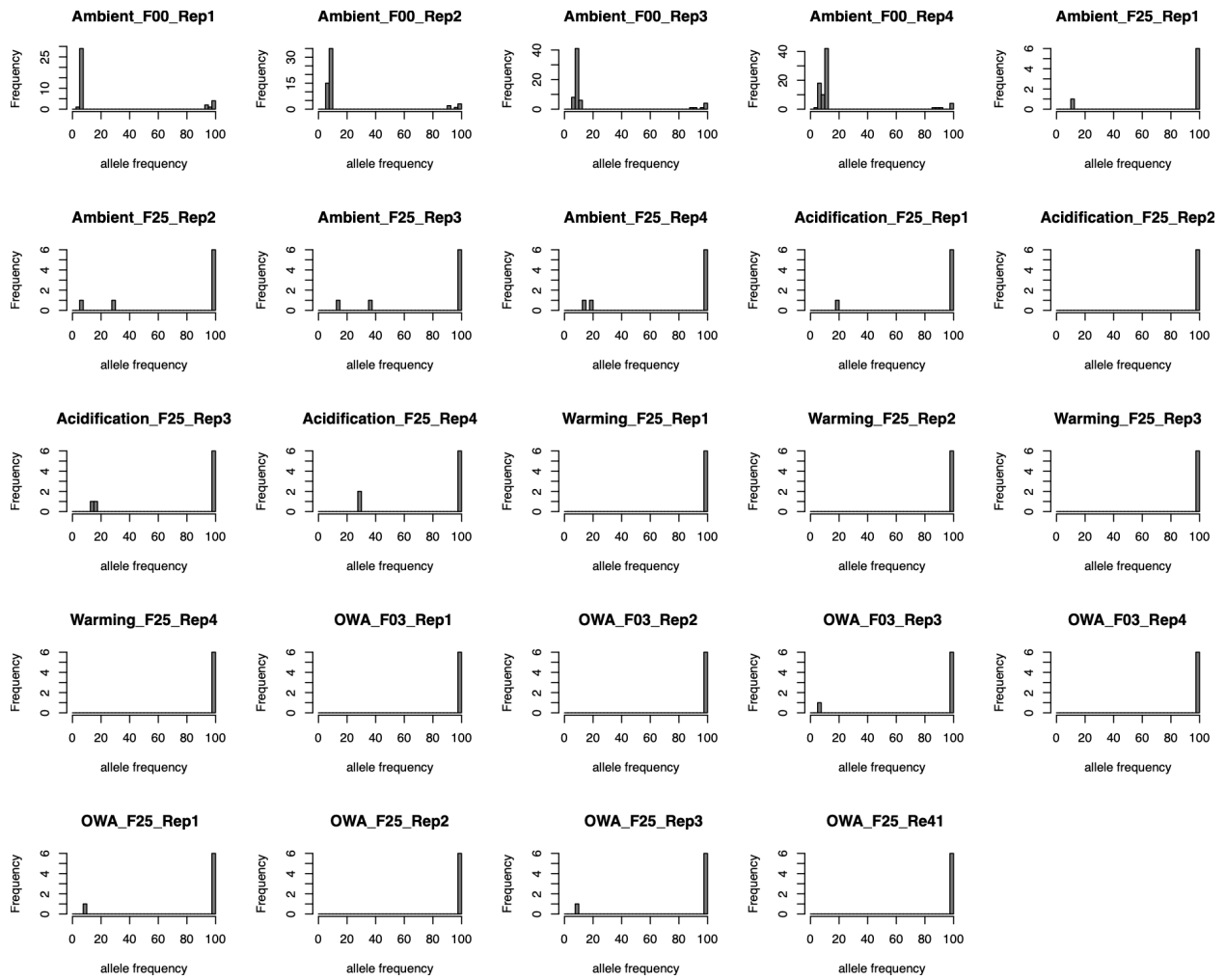


Figure S9: Frequency of mitochondrial haplotypes. Histograms show the frequency of haplotypes from variants in the pooled data. At F0, there were low frequency variants present in the data, indicating the presence of a low frequency haplotype. These minor alleles drop out by F3 and nearly absent by F25 across all samples. This indicates that the vast majority of samples matched the reference genome after 3 generations of selection. Given the low starting frequency of minor mitochondrial haplotypes, this suggests the pooled samples likely consisted of a dominant mitochondrial haplotype and selection across the rest of the genome was likely not due to shifting frequencies of mitochondrial clades.

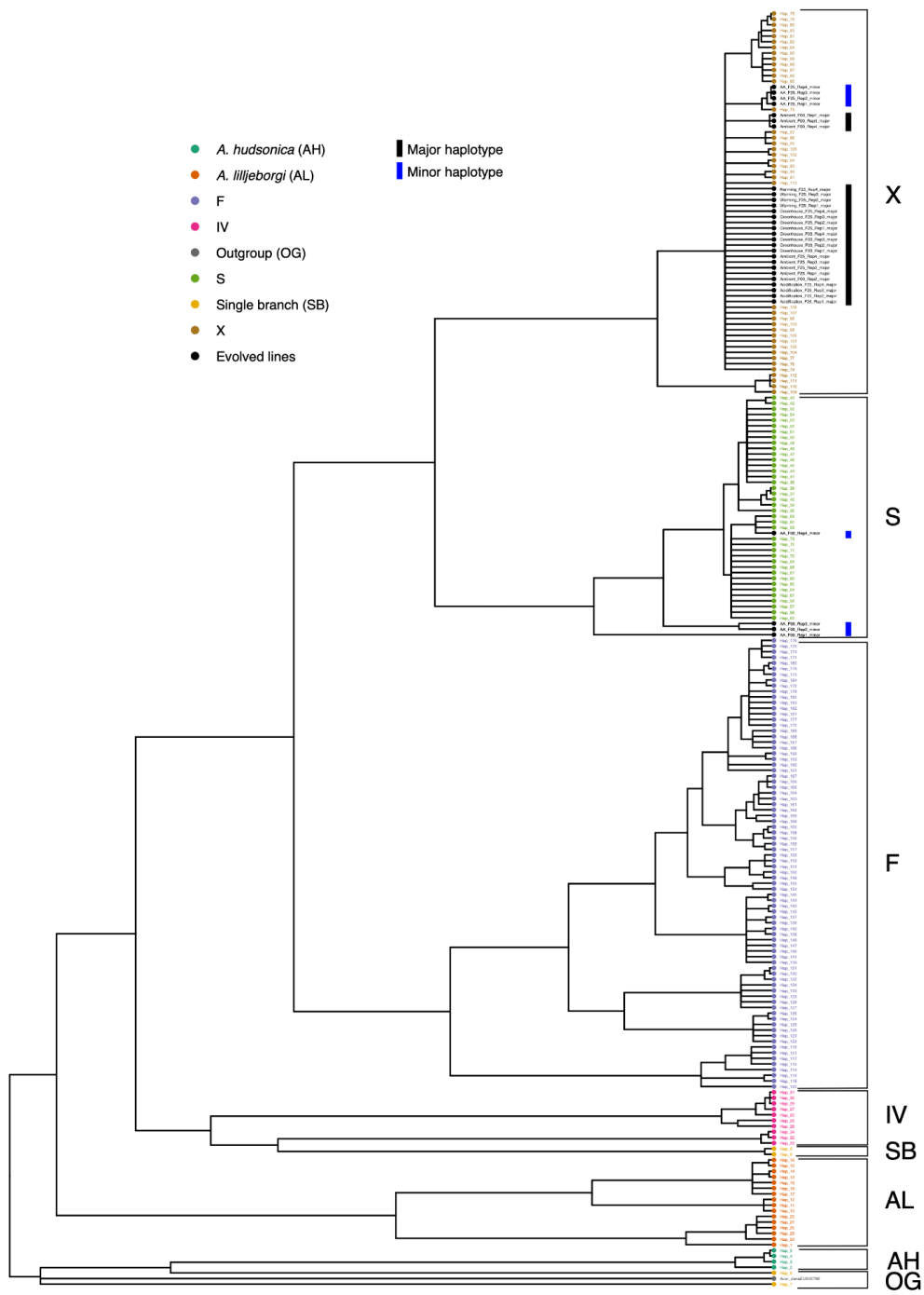


Figure S10: Phylogenetic tree from COI sequence data. We determined the clade of samples from this study using samples from Figueroa et al. (2020). Black and blue bars are the tree tips indicate major and minor haplotypes in the pooled samples, respectively. Samples in our study were predominantly clade X.

Supplemental References:

1. G. Chen, M. P. Hare, Cryptic ecological diversification of a planktonic estuarine copepod, *Acartia tonsa*. *Mol. Ecol.* **17**, 1451–1468 (2008).
2. G. Chen, M. P. Hare, Cryptic diversity and comparative phylogeography of the estuarine copepod *Acartia tonsa* on the US Atlantic coast. *Mol. Ecol.* **20**, 2425–2441 (2011).
3. N. J. Figueroa, D. F. Figueroa, D. Hicks, Phylogeography of *Acartia tonsa* Dana, 1849 (Calanoida: Copepoda) and phylogenetic reconstruction of the genus *Acartia* Dana, 1846. *Mar. Biodivers.* **50**, 23 (2020).
4. D. C. Koboldt, *et al.*, VarScan 2: somatic mutation and copy number alteration discovery in cancer by exome sequencing. *Genome Res.* **22**, 568–576 (2012).
5. R. C. Edgar, MUSCLE: a multiple sequence alignment method with reduced time and space complexity. *BMC Bioinformatics* **5**, 113 (2004).
6. E. Paradis, J. Claude, K. Strimmer, APE: Analyses of Phylogenetics and Evolution in R language. *Bioinformatics* **20**, 289–290 (2004).
7. F. Ronquist, *et al.*, MrBayes 3.2: efficient Bayesian phylogenetic inference and model choice across a large model space. *Syst. Biol.* **61**, 539–542 (2012).
8. G. Yu, D. K. Smith, H. Zhu, Y. Guan, T. T. Lam, Ggtree : An r package for visualization and annotation of phylogenetic trees with their covariates and other associated data. *Methods Ecol. Evol.* **8**, 28–36 (2017).
9. V. Buffalo, G. Coop, Estimating the genome-wide contribution of selection to temporal allele frequency change. *Proc. Natl. Acad. Sci. U. S. A.* **117**, 20672–20680 (2020).

Supplemental table 2: Go enrichment of candidate SNPs from topGO. The group column indicates the set of SNPs in the enrichment test. “_all” means all significant loci for that treatment were tested. “_unique” means only those SNPs unique to that treatment. When multiple treatments are listed this indicates SNP sets that are significant under multiple treatments.

GO.ID	Term	Annotated	Significant	Expected	classicFisher	weight	group
GO:0019674	NAD metabolic process NADP biosynthetic process	8	7	1.91	0.00028	0.00028	OWA_all
GO:0006741		9	7	2.15	0.00098	0.00098	OWA_all
GO:0000470	maturation of LSU-rRNA maturation of LSU-rRNA from tricistronic...	14	11	3.35	2.40E-05	0.00316	OWA_all
GO:0000463	positive regulation of DNA-templated tra... regulation of Ras	6	5	1.43	0.00371	0.00371	OWA_all
GO:0032786	protein signal transdu... imaginal disc-derived	6	5	1.43	0.00371	0.00371	OWA_all
GO:0046578	leg morphogenesis proximal/distal pattern formation	12	7	2.87	0.01087	0.01087	OWA_all
GO:0007480	viral mRNA export from host cell nucleus	5	4	1.19	0.01311	0.01311	OWA_all
GO:0009954	positive regulation of cell growth invol... vascular associat...	5	4	1.19	0.01311	0.01311	OWA_all
GO:0046784	negative regulation of DNA damage checkp... inorganic ion homeostasis	5	4	1.19	0.01311	0.01311	OWA_all
GO:0061051	homeostasis of number of cells	38	12	9.08	0.17563	0.01356	OWA_all
GO:1904707	DNA conformation change	26	8	6.21	0.26785	0.01363	OWA_all
GO:2000002	translation	27	8	6.45	0.30702	0.01365	OWA_all
GO:0098771	ribosomal large subunit assembly	243	61	58.07	0.34741	0.01544	OWA_all
GO:0048872	ribosomal small subunit assembly	10	6	2.39	0.0156	0.0156	OWA_all
GO:0000028	small GTPase mediated signal transductio...	10	6	2.39	0.0156	0.0156	OWA_all
GO:0007264	proteolysis positive regulation of cell growth	53	21	12.67	0.00739	0.01888	OWA_all
GO:0006508	mitochondrion organization	169	46	40.39	0.17002	0.02514	OWA_all
GO:0030307	imaging disc pattern formation	11	8	2.63	0.00084	0.03143	OWA_all
GO:0007005	regulation of cell size	46	12	10.99	0.41878	0.03164	OWA_all
GO:0007447		6	4	1.43	0.03192	0.03192	OWA_all
GO:0008361		9	5	2.15	0.04058	0.04058	OWA_all

	positive regulation of						
GO:2000573	DNA biosynthetic ...	9	5	2.15	0.04058	0.04058	OWA_all
GO:0000460	maturation of 5.8S rRNA	10	6	2.39	0.0156	0.04438	OWA_all
GO:0000154	rRNA modification	11	5	2.63	0.09728	0.04462	OWA_all
GO:0030833	regulation of actin						
	filament polymerizat...	11	5	2.63	0.09728	0.04462	OWA_all
GO:0045862	positive regulation of						
	proteolysis	24	8	5.74	0.19474	0.04464	OWA_all
GO:0007088	regulation of mitotic						
	nuclear division	15	6	1.24	0.00078	0.00035	ambient_all
GO:0007059	chromosome						
	segregation	32	7	2.64	0.01336	0.00035	ambient_all
GO:0120036	plasma membrane						
	bounded cell projection						
	...	86	9	7.1	0.2761	0.00056	ambient_all
GO:0000082	G1/S transition of						
	mitotic cell cycle	13	5	1.07	0.00271	0.00271	ambient_all
	mitotic spindle						
GO:0007052	organization	13	5	1.07	0.00271	0.00271	ambient_all
GO:0051225	spindle assembly						
	phosphatidylinositol	13	5	1.07	0.00271	0.00271	ambient_all
GO:0006661	biosynthetic proces...						
	purine ribonucleoside	11	5	0.91	0.00112	0.0048	ambient_all
GO:0009168	monophosphate bios...						
	...	5	3	0.41	0.00489	0.00489	ambient_all
GO:0006468	protein phosphorylation						
	sensory organ	163	19	13.45	0.07378	0.00659	ambient_all
GO:0007423	development						
	...	64	9	5.28	0.07661	0.00905	ambient_all
GO:0046033	AMP metabolic process						
	actin filament bundle	6	3	0.5	0.00919	0.00919	ambient_all
GO:0051017	assembly						
	positive regulation of	6	3	0.5	0.00919	0.00919	ambient_all
GO:0043547	GTPase activity						
	anatomical structure	24	6	1.98	0.0112	0.0112	ambient_all
GO:0048856	development						
	...	448	44	36.97	0.11107	0.01407	ambient_all
GO:1902600	proton transmembrane						
	transport	26	6	2.15	0.01667	0.01667	ambient_all
GO:0045785	positive regulation of						
	cell adhesion	11	5	0.91	0.00112	0.01884	ambient_all
GO:0022409	positive regulation of						
	cell-cell adhesio...	8	3	0.66	0.02274	0.02274	ambient_all
GO:0003002	regionalization						
	...	46	7	3.8	0.07983	0.02961	ambient_all
GO:1902905	positive regulation of						
	supramolecular fi...	11	4	0.91	0.00937	0.03594	ambient_all
GO:0001501	skeletal system						
	...	12	4	0.99	0.01316	0.03597	ambient_all
GO:0110053	development						
	regulation of actin						
	...	15	4	1.24	0.02981	0.03605	ambient_all
GO:0000460	filament organizatio...						
	maturation of 5.8S rRNA	10	3	0.83	0.04308	0.03623	ambient_all
GO:0007276	...						
	gamete generation	67	5	5.53	0.66016	0.03709	ambient_all

GO:0022412	cellular process involved in reproduction	57	4	4.7	0.70529	0.03714	ambient_all
GO:0001701	in utero embryonic development	16	4	1.32	0.03725	0.03725	ambient_all
GO:0033365	protein localization to organelle	58	5	1.88	0.0382	0.00019	acidification_all
GO:0009060	aerobic respiration proton transmembrane transport	21	4	0.68	0.0041	0.00407	acidification_all
GO:1902600		26	4	0.84	0.009	0.00899	acidification_all
GO:0008354	germ cell migration negative regulation of endopeptidase activity	5	2	0.16	0.0098	0.00979	acidification_all
GO:0010951	apical protein localization	5	2	0.16	0.0098	0.00979	acidification_all
GO:0045176	sodium ion transport	18	3	0.58	0.019	0.01899	acidification_all
GO:0006814	primary metabolic process	1489	49	48.37	0.4904	0.02897	acidification_all
GO:0044238	monovalent inorganic cation homeostasis	8	2	0.26	0.0257	0.0322	acidification_all
GO:0055067	enzyme linked receptor protein signaling pathway	43	3	1.4	0.1621	0.03225	acidification_all
GO:0007167	imaginal disc development	36	2	1.17	0.3277	0.03254	acidification_all
GO:0007444	establishment or maintenance of transmembrane protein localization	10	2	0.32	0.0396	0.03963	acidification_all
GO:0010248	mitotic spindle organization	13	8	2.37	0.00064	0.00021	warming_all
GO:0007052	actin filament bundle assembly	6	5	1.1	0.00102	0.00102	warming_all
GO:0051017	chromosome segregation	32	8	5.84	0.21677	0.00188	warming_all
GO:0007059	primary metabolic process	1489	294	271.8	0.01459	0.0029	warming_all
GO:0044238	ribosomal small subunit assembly	13	7	2.37	0.00403	0.003	warming_all
GO:0051225	imaginal disc-derived wing morphogenesis	10	6	1.83	0.00389	0.00389	warming_all
GO:0000028	leg morphogenesis	23	10	4.2	0.00441	0.00397	warming_all
GO:0007476	proximal/distal pattern formation	5	4	0.91	0.0047	0.0047	warming_all
GO:0001947	positive regulation of heart looping	5	4	0.91	0.0047	0.0047	warming_all
GO:0007480	imperial disc-derived proximal/distal pattern formation	5	4	0.91	0.0047	0.0047	warming_all
GO:0009954	homeostasis of number of cells	5	4	0.91	0.0047	0.0047	warming_all
GO:0043280	kidney epithelium development	26	9	4.75	0.03471	0.00599	warming_all
GO:0048872		10	6	1.83	0.00389	0.00599	warming_all
GO:0072073							

	plasma membrane bounded cell projection							
GO:0120036	...	86	16	15.7	0.51172	0.00614	warming_all	
GO:0030324	lung development regulation of small molecule metabolic p...	8	5	1.46	0.00686	0.00686	warming_all	
GO:0062012	molecule metabolic p...	28	8	5.11	0.1226	0.0069	warming_all	
GO:0042060	wound healing positive regulation of protein phosphory...	11	6	2.01	0.00724	0.00724	warming_all	
GO:0001934	imaginal disc pattern formation	23	7	4.2	0.10995	0.00734	warming_all	
GO:0007447	regulation of generation of precursor me...	6	4	1.1	0.01208	0.01208	warming_all	
GO:0043467	cell-cell signaling regulation of Ras	106	22	19.36	0.28524	0.0121	warming_all	
GO:0046578	protein signal transdu...	12	6	2.19	0.01229	0.01229	warming_all	
GO:0007088	regulation of mitotic nuclear division	15	6	2.74	0.04077	0.01315	warming_all	
GO:0044260	cellular macromolecule metabolic process	1030	214	188.0	0.00465	0.01327	warming_all	
GO:0018108	peptidyl-tyrosine phosphorylation	19	8	3.47	0.01339	0.01919	warming_all	
GO:0000082	G1/S transition of mitotic cell cycle	13	6	2.37	0.01936	0.01936	warming_all	
GO:0032501	multicellular organismal process	512	96	93.49	0.39616	0.01956	warming_all	
GO:0043547	positive regulation of GTPase activity	24	9	4.38	0.02042	0.02042	warming_all	
GO:0110053	regulation of actin filament organizatio...	15	8	2.74	0.00226	0.02056	warming_all	
GO:0045862	positive regulation of proteolysis	24	9	4.38	0.02042	0.02064	warming_all	
GO:1902905	positive regulation of supramolecular fi...	11	6	2.01	0.00724	0.02072	warming_all	
GO:0050769	positive regulation of neurogenesis	17	7	3.1	0.02336	0.02073	warming_all	
GO:0042692	muscle cell differentiation	37	6	6.76	0.69306	0.0213	warming_all	
GO:0048856	anatomical structure development	448	91	81.8	0.12256	0.0228	warming_all	
GO:0048546	digestive tract morphogenesis	12	7	2.19	0.0022	0.02379	warming_all	
GO:0007163	establishment or maintenance of cell	pol...	24	8	4.38	0.05619	0.024	warming_all
GO:0071456	cellular response to hypoxia	7	4	1.28	0.02415	0.02415	warming_all	
GO:0043161	proteasome-mediated ubiquitin-dependent ...	44	12	8.03	0.09052	0.02576	warming_all	
GO:0006468	protein phosphorylation	163	45	29.76	0.00159	0.02795	warming_all	

	RNA biosynthetic process	334	73	60.99	0.04266	0.03168	warming_all
GO:0032774	regulation of nitrogen compound metabolism	429	88	78.33	0.1066	0.03199	warming_all
GO:0051171	microtubule cytoskeleton organization involved in positive regulation of phosphorylation	15	10	2.74	4.70E-05	0.03252	warming_all
GO:1902850	regulation of protein targeting	26	9	4.75	0.03471	0.03293	warming_all
GO:0042327	protein lipidation regulation of cellular component movement	7	5	1.28	0.00302	0.033	warming_all
GO:1903533	protein acylation	8	5	1.46	0.00686	0.03303	warming_all
GO:0006497	reproduction	25	8	4.56	0.06997	0.03304	warming_all
GO:0051270	telomere organization regulation of carbohydrate metabolic process	17	6	3.1	0.07303	0.03311	warming_all
GO:0043543	regulation of catabolic process	118	23	21.55	0.39957	0.03331	warming_all
GO:0000003	response to other organism	12	3	2.19	0.37954	0.0334	warming_all
GO:0032200	vascular process in circulatory system	24	5	4.38	0.4528	0.03343	warming_all
GO:0006109	hexose metabolic process	54	10	9.86	0.53657	0.03349	warming_all
GO:0009894	organic substance catabolic process	61	11	11.14	0.57173	0.03353	warming_all
GO:0051707	regulation of protein stability	18	3	3.29	0.66498	0.03355	warming_all
GO:0003018	metal ion homeostasis	30	5	5.48	0.66385	0.03358	warming_all
GO:0019318	microtubule-based process	192	34	35.06	0.61257	0.03368	warming_all
GO:1901575	regulation of protein targeting	29	4	5.3	0.80372	0.03369	warming_all
GO:0055065	chloride transport	68	18	12.42	0.05763	0.03427	warming_all
GO:0007017	inflammatory response	20	7	3.65	0.0567	0.03493	warming_all
GO:0031647	cell fate specification	14	6	2.56	0.02878	0.04119	warming_all
GO:0006997	proteasome assembly	8	4	1.46	0.04144	0.04144	warming_all
GO:0006821	regulation of body fluid levels	8	4	1.46	0.04144	0.04144	warming_all
GO:0043248	positive regulation of cytoskeleton organization	8	4	1.46	0.04144	0.04144	warming_all
GO:0050878	mRNA processing	100	21	18.26	0.27173	0.04378	warming_all
GO:0006954	salivary gland morphogenesis	12	6	2.19	0.01229	0.04484	warming_all
GO:0006397	positive regulation of morphogenesis	206	41	37.62	0.29006	0.0449	warming_all
GO:0007435	tissue homeostasis	10	4	1.83	0.09187	0.04524	warming_all
GO:0001894	inflammatory response	5	3	0.91	0.04527	0.04527	warming_all

GO:0007440	foregut morphogenesis	5	3	0.91	0.04527	0.04527	warming_all
GO:0007492	endoderm development	5	3	0.91	0.04527	0.04527	warming_all
GO:0031507	heterochromatin assembly	5	3	0.91	0.04527	0.04527	warming_all
GO:1903053	regulation of extracellular matrix	5	3	0.91	0.04527	0.04527	warming_all
GO:1903955	organ... positive regulation of protein targeting...	5	3	0.91	0.04527	0.04527	warming_all
GO:0007612	learning inorganic ion transmembrane	12	4	2.19	0.16089	0.04534	warming_all
GO:0098660	transport respiratory electron	71	14	12.96	0.4219	0.04553	warming_all
GO:0022904	transport chain oxidative	13	2	0.03	0.00045	0.00045	ambient_acidification
GO:0006119	phosphorylation erythrocyte	14	2	0.04	0.00053	0.00053	ambient_acidification
GO:0030218	differentiation actin filament bundle	11	3	0.19	0.00071	0.00071	ambient_warming
GO:0051017	assembly	6	2	0.1	0.00414	0.00414	ambient_warming
GO:0042060	wound healing positive regulation of	11	2	0.19	0.01439	0.01439	ambient_warming
GO:0045785	cell adhesion positive regulation of	11	2	0.19	0.01439	0.01439	ambient_warming
GO:1902905	supramolecular fi...	11	2	0.19	0.01439	0.01439	ambient_warming
GO:0048285	organelle fission	48	7	0.82	1.20E-05	0.0152	ambient_warming
GO:0006412	translation positive regulation of	243	9	4.17	0.01992	0.0157	ambient_warming
GO:0051495	cytoskeleton orga...	12	2	0.21	0.01708	0.01708	ambient_warming
GO:0043401	steroid hormone mediated signaling pathw...	13	2	0.22	0.01996	0.01996	ambient_warming
GO:0110053	regulation of actin filament organizatio...	15	2	0.26	0.0263	0.0263	ambient_warming
GO:0050896	response to stimulus transcription initiation	619	13	10.63	0.24958	0.02861	ambient_warming
GO:0006367	from RNA polyme...	18	2	0.31	0.03709	0.03709	ambient_warming
GO:0006814	sodium ion transport response to oxidative	18	2	0.31	0.03709	0.03709	ambient_warming
GO:0006979	stress purine ribonucleoside	21	2	0.36	0.04928	0.04928	ambient_warming
GO:0009168	monophosphate bios...	5	2	0.03	0.00025	0.00025	ambient_OWA
GO:0046033	AMP metabolic process	6	2	0.03	0.00038	0.00038	ambient_OWA
GO:0009152	purine ribonucleotide biosynthetic proce...	41	2	0.21	0.01853	0.01853	ambient_OWA
GO:0006508	acidification_warmi proteolysis	169	2	0.25	0.022	0.022	ng
GO:0046331	lateral inhibition	13	2	0.03	0.00045	0.00045	acidification_OWA

GO:0000398	mRNA splicing, via spliceosome regulation of Ras	77	2	0.2	0.01561	0.01561	acidification_OWA
GO:0046578	protein signal transduction, positive regulation of	12	5	1.07	0.0025	0.0025	warming_OWA
GO:0045862	proteolysis regulation of small molecule metabolic process	24	5	2.13	0.0557	0.0026	warming_OWA
GO:0062012	molecule metabolic process	28	6	2.49	0.0329	0.0032	warming_OWA
GO:0006397	mRNA processing, imaginal disc-derived	100	12	8.89	0.1727	0.0048	warming_OWA
GO:0007480	leg morphogenesis, RNA biosynthetic process	5	3	0.44	0.0061	0.0061	warming_OWA
GO:0032774	telomere organization, regulation of carbohydrate metabolic process	334	40	29.68	0.0249	0.0072	warming_OWA
GO:0032200	reproduction	12	3	1.07	0.0836	0.0079	warming_OWA
GO:0006109	metal ion homeostasis, hexose metabolic process	24	4	2.13	0.1587	0.0079	warming_OWA
GO:0000003	regulation of catabolic process	118	12	10.49	0.3551	0.0079	warming_OWA
GO:0055065	regulation of transcription, DNA-templated	29	4	2.58	0.2539	0.0079	warming_OWA
GO:0019318	regulation of gene expression, cellular lipid metabolic process	30	4	2.67	0.2742	0.0079	warming_OWA
GO:0009894	positive regulation of protein phosphorylation, microtubule-based process	54	6	4.8	0.3465	0.0079	warming_OWA
GO:0006355	microtubule-based process	307	36	27.28	0.0435	0.0098	warming_OWA
GO:0007447	protein targeting to membrane	6	3	0.53	0.0113	0.0113	warming_OWA
GO:0043467	membrane lipid metabolic process	6	3	0.53	0.0113	0.0113	warming_OWA
GO:0045815	membrane lipid metabolic process	6	3	0.53	0.0113	0.0113	warming_OWA
GO:0044255	membrane lipid metabolic process	72	11	6.4	0.0502	0.0166	warming_OWA
GO:0001933	membrane lipid metabolic process	21	5	1.87	0.0331	0.0169	warming_OWA
GO:0007017	membrane lipid metabolic process	68	7	6.04	0.4008	0.0175	warming_OWA
GO:0006493	membrane lipid metabolic process	7	3	0.62	0.0185	0.0185	warming_OWA
GO:1901564	membrane lipid metabolic process	881	96	78.3	0.007	0.0211	warming_OWA
GO:0006643	membrane lipid metabolic process	9	3	0.8	0.0389	0.0221	warming_OWA
GO:0006612	membrane lipid metabolic process	13	3	1.16	0.1019	0.0222	warming_OWA
GO:1901071	membrane lipid metabolic process	18	3	1.6	0.211	0.0223	warming_OWA
GO:0016358	dendrite development	26	3	2.31	0.4108	0.0224	warming_OWA

	establishment or maintenance of cell						
GO:0007163	pol...	24	6	2.13	0.0158	0.0225	warming_OWA
GO:0006915	apoptotic process regulation of protein-containing complex...	78	8	6.93	0.3902	0.0234	warming_OWA
GO:0043254		31	8	2.76	0.0045	0.0268	warming_OWA
GO:0006909	phagocytosis negative regulation of	20	5	1.78	0.0271	0.0271	warming_OWA
GO:1902532	intracellular sig...	20	5	1.78	0.0271	0.0271	warming_OWA
GO:0006997	nucleus organization regulation of body fluid	14	4	1.24	0.0298	0.0276	warming_OWA
GO:0050878	levels	8	3	0.71	0.0277	0.0277	warming_OWA
GO:0015986	ATP synthesis coupled proton transport organic substance	14	4	1.24 138.2	0.0298	0.0298	warming_OWA
GO:0071704	metabolic process	1556	158	9	0.0038	0.0378	warming_OWA
GO:0008361	regulation of cell size regulation of mRNA	9	3	0.8	0.0389	0.0389	warming_OWA
GO:0043488	stability	9	3	0.8	0.0389	0.0389	warming_OWA
GO:0023051	regulation of signaling regulation of actin	151	20	13.42	0.0421	0.0401	warming_OWA
GO:0030833	filament polymeriz... regulation of reactive	11	4	0.98	0.0122	0.0414	warming_OWA
GO:2000377	oxygen species me... regulation of mitotic	12	4	1.07	0.017	0.0414	warming_OWA
GO:0007088	nuclear division chromosome	15	6	0.96	0.0002	0.0001	ambient_unique
GO:0007059	segregation G1/S transition of	32	6	2.06	0.01437	0.00011	ambient_unique
GO:0000082	mitotic cell cycle mitotic spindle	13	5	0.83	0.00087	0.00087	ambient_unique
GO:0007052	organization	13	5	0.83	0.00087	0.00087	ambient_unique
GO:0051225	spindle assembly purine ribonucleoside	13	5	0.83	0.00087	0.00087	ambient_unique
GO:0009168	monophosphate bios... positive regulation of	5	3	0.32	0.00237	0.00237	ambient_unique
GO:0043547	GTPase activity	24	6	1.54	0.00327	0.00327	ambient_unique
GO:0046033	AMP metabolic process anatomical structure	6	3	0.39	0.00451	0.00451	ambient_unique
GO:0048856	development positive regulation of	448	31	28.77	0.35119	0.00755	ambient_unique
GO:0022409	cell-cell adhesio...	8	3	0.51	0.01147	0.01147	ambient_unique
GO:0006468	protein phosphorylation	163	15	10.47	0.09607	0.01493	ambient_unique
GO:0000460	maturation of 5.8S rRNA	10	3	0.64	0.02234	0.02243	ambient_unique
GO:0007276	gamete generation organic substance	67	4	4.3	0.63412	0.02311	ambient_unique
GO:0071704	metabolic process phosphatidylinositol	1556	95	99.94	0.80771	0.03364	ambient_unique
GO:0006661	biosynthetic proces...	11	4	0.71	0.0038	0.03542	ambient_unique

GO:0001894	tissue homeostasis	5	2	0.32	0.03606	0.03606	ambient_unique
GO:0010842	retina layer formation regulation of TOR signaling	5	2	0.32	0.03606	0.03606	ambient_unique
GO:0032006	protein localization to organelle	5	2	0.32	0.03606	0.03606	ambient_unique
GO:0033365		58	4	1	0.0164	0.00052	acidification_unique
GO:0008354	germ cell migration apical protein localization	5	2	0.09	0.0028	0.00279	acidification_unique
GO:0045176		5	2	0.09	0.0028	0.00279	acidification_unique
GO:0006814	sodium ion transport establishment or maintenance of transmem...	18	3	0.31	0.0032	0.00323	acidification_unique
GO:0010248		10	2	0.17	0.0119	0.0119	acidification_unique
GO:0007612	learning peptidyl-tyrosine dephosphorylation	12	2	0.21	0.0171	0.01708	acidification_unique
GO:0035335	regulation of reactive oxygen species me...	12	2	0.21	0.0171	0.01708	acidification_unique
GO:2000377		12	2	0.21	0.0171	0.01708	acidification_unique
GO:0016925	protein sumoylation oxidative phosphorylation	13	2	0.22	0.02	0.01996	acidification_unique
GO:0006119	negative regulation of cellular developmental process	14	2	0.24	0.023	0.02304	acidification_unique
GO:0043066		40	3	0.69	0.0301	0.03008	acidification_unique
GO:0048869	process	276	9	4.74	0.0415	0.04668	acidification_unique
GO:0009060	aerobic respiration regulation of mitotic cell cycle phase t...	21	2	0.36	0.0493	0.04928	acidification_unique
GO:1901990	homeostasis of number of cells	18	2	0.31	0.0371	0.04986	acidification_unique
GO:0048872	cellular macromolecule metabolic process	26	7	2.91	0.0207	0.0014	warming_unique
GO:0044260	proteasome-mediated ubiquitin-dependent ...	1030	131	115.3	0.029	0.0018	warming_unique
GO:0043161	regulation of protein stability	44	11	4.93	0.0074	0.0043	warming_unique
GO:0031647	positive regulation of neurogenesis	20	6	2.24	0.0187	0.0045	warming_unique
GO:0050769	muscle cell differentiation	17	7	1.9	0.0015	0.005	warming_unique
GO:0042692	response to mechanical stimulus	37	6	4.14	0.2281	0.0051	warming_unique
GO:0009612		12	5	1.34	0.0069	0.0069	warming_unique
GO:0006997	nucleus organization	14	5	1.57	0.0145	0.0075	warming_unique
GO:0006821	chloride transport	8	4	0.9	0.0075	0.0075	warming_unique
GO:0030324	lung development	8	4	0.9	0.0075	0.0075	warming_unique
GO:0043248	proteasome assembly	8	4	0.9	0.0075	0.0075	warming_unique

	multicellular organismal process	512	58	57.36	0.4861	0.0107	warming_unique
GO:0032501	salivary gland morphogenesis	10	4	1.12	0.0187	0.0117	warming_unique
GO:0007435	heart looping heterochromatin assembly	5	3	0.56	0.0117	0.0117	warming_unique
GO:0001947	positive regulation of protein targeting...	5	3	0.56	0.0117	0.0117	warming_unique
GO:0031507	RNA processing	206	23	23.08	0.5429	0.012	warming_unique
GO:1903955	cell-cell adhesion	19	7	2.13	0.0032	0.012	warming_unique
GO:0006396	nucleosome assembly multicellular organism growth	9	4	1.01	0.0123	0.0123	warming_unique
GO:0006334	microtubule cytoskeleton organization in...	9	4	1.01	0.0123	0.0123	warming_unique
GO:0035264	telomere organization	15	5	1.68	0.0198	0.0124	warming_unique
GO:0032200	regulation of cell shape	12	3	1.34	0.143	0.0125	warming_unique
GO:0008360	spermatid development determination of adult lifespan	14	5	1.57	0.0145	0.0145	warming_unique
GO:0007286	cellular catabolic process	10	4	1.12	0.0187	0.0187	warming_unique
GO:0008340	GPI anchor biosynthetic process	10	4	1.12	0.0187	0.0187	warming_unique
GO:0044248	Arp2/3 complex-mediated actin nucleation	187	26	20.95	0.1377	0.0209	warming_unique
GO:0006506	microtubule-based process	6	3	0.67	0.0215	0.0215	warming_unique
GO:0034314	wound healing anatomical structure development	68	12	7.62	0.0714	0.0264	warming_unique
GO:0007017	chromatin organization protein N-linked glycosylation signal transduction by protein phosphorylation	11	4	1.23	0.0269	0.0269	warming_unique
GO:0042060	head development kidney epithelium development	448	55	50.19	0.2373	0.0336	warming_unique
GO:0006325	autophagy	71	12	7.95	0.0928	0.034	warming_unique
GO:0006487	positive regulation of epithelial cell proliferation	12	5	1.34	0.0069	0.0341	warming_unique
GO:0023014	molting cycle, chitin-based cuticle	29	7	3.25	0.0367	0.0343	warming_unique
GO:0006914	head development positive regulation of epithelial cell proliferation	42	8	4.71	0.0901	0.0344	warming_unique
GO:0060322	development	10	4	1.12	0.0187	0.0345	warming_unique
GO:0072073	protein targeting...	7	3	0.78	0.0346	0.0346	warming_unique
GO:0050679	chitosan metabolic process	9	3	1.01	0.07	0.0347	warming_unique
GO:0007591	cell wall biogenesis						

	regulation of cell morphogenesis						
GO:0010769	involve... negative regulation of Wnt signaling pat...	9	3	1.01	0.07	0.0347	warming_unique
GO:0030178	tube formation	11	3	1.23	0.1164	0.0347	warming_unique
GO:0035148	cellular protein localization	15	3	1.68	0.2317	0.0348	warming_unique
GO:0034613	open tracheal system development	118	13	13.22	0.5715	0.0352	warming_unique
GO:0007424	cellular lipid metabolic process	24	6	2.69	0.0442	0.0366	warming_unique
GO:0044255	imaginal disc-derived wing morphogenesis	72	11	8.07	0.1759	0.0367	warming_unique
GO:0007476	peptidyl-tyrosine phosphorylation	23	7	2.58	0.0103	0.0477	warming_unique
GO:0018108	NADP biosynthetic process	19	5	2.13	0.053	0.0485	warming_unique
GO:0006741	maturation of LSU-rRNA positive regulation of DNA-templated tra...	9	7	1.67	0.00019	0.00019	OWA_unique
GO:0000470	translation ribosomal small subunit assembly	14	10	2.6	2.20E-05	0.00077	OWA_unique
GO:0032786	viral mRNA export from host cell nucleus	6	5	1.11	0.0011	0.0011	OWA_unique
GO:0006412	positive regulation of cell growth invol...	243	51	45.1	0.17439	0.00212	OWA_unique
GO:0000028	positive regulation of vascular associat...	10	6	1.86	0.00423	0.00423	OWA_unique
GO:0046784	negative regulation of DNA damage checkp...	5	4	0.93	0.00501	0.00501	OWA_unique
GO:0061051	homeostasis of number of cells	5	4	0.93	0.00501	0.00501	OWA_unique
GO:1904707	maturation of 5.8S rRNA	26	7	4.83	0.19349	0.00637	OWA_unique
GO:2000002	maturation of LSU-rRNA from tricistronic...	6	4	1.11	0.01282	0.01282	OWA_unique
GO:0048872	positive regulation of DNA biosynthetic ...	9	5	1.67	0.01409	0.01409	OWA_unique
GO:0000463	maturation of 5.8S rRNA homeostasis of number of cells	10	6	1.86	0.00423	0.02168	OWA_unique
GO:0000460	rRNA modification	11	5	2.04	0.03736	0.02183	OWA_unique
GO:0000154	ribosomal large subunit assembly	10	5	1.86	0.02395	0.02395	OWA_unique
GO:0000027	cellular component biogenesis	302	67	56.05	0.05229	0.03294	OWA_unique
GO:0044085	regulation of nitrogen compound metaboli...	429	85	79.62	0.25234	0.03376	OWA_unique
GO:0051171	exocrine system development	14	8	2.6	0.0014	0.03386	OWA_unique
GO:0035272	embryonic heart tube development	8	3	1.48	0.17198	0.0344	OWA_unique
GO:0035050	cellular ion homeostasis	34	7	6.31	0.44829	0.03452	OWA_unique

	regulation of response to stimulus	173	32	32.11	0.54152	0.03464	OWA_unique
GO:0006813	potassium ion transport	28	8	5.2	0.1317	0.03542	OWA_unique
GO:0000469	cleavage involved in rRNA processing	11	5	2.04	0.03736	0.03736	OWA_unique
GO:0051094	positive regulation of developmental process	54	14	10.02	0.11192	0.04331	OWA_unique
GO:0000245	spliceosomal complex assembly	15	6	2.78	0.0438	0.0438	OWA_unique
GO:0007435	salivary gland morphogenesis	10	5	1.86	0.02395	0.04701	OWA_unique
GO:0009954	proximal/distal pattern formation	5	3	0.93	0.04729	0.04729	OWA_unique
GO:0030166	proteoglycan biosynthetic process	5	3	0.93	0.04729	0.04729	OWA_unique
GO:0015698	inorganic anion transport	13	4	2.41	0.2093	0.04741	OWA_unique
GO:0001822	kidney development	29	5	5.38	0.64799	0.04792	OWA_unique
GO:0007264	small GTPase mediated signal transduction	53	13	9.84	0.16964	0.048	OWA_unique
GO:0098660	inorganic ion transmembrane transport	71	9	13.18	0.93185	0.04894	OWA_unique
GO:0090304	nucleic acid metabolic process	677	3	0.76	0.016	0.0021	ambient_acidification_on_OWA
GO:0006367	transcription initiation from RNA polymerase II promoter	18	2	0.11	0.0048	0.0048	ambient_warming_OWA
GO:0043161	proteasome-mediated ubiquitin-dependent protein catabolic process	44	2	0.26	0.0274	0.0274	ambient_warming_OWA
GO:0009260	ribonucleotide biosynthetic process	43	2	0.19	0.015	0.0083	acidification_warming_OWA
GO:0023051	ubiquitin-dependent protein catabolic process	151	3	0.68	0.0265	0.0235	acidification_warming_OWA
GO:0043170	macromolecule metabolic process	1313	10	7.84	0.204	0.0038	ambient_acidification_on_warming_OWA
GO:0090304	nucleic acid metabolic process	677	5	4.04	0.38	0.0044	ambient_acidification_on_warming_OWA
GO:0044238	primary metabolic process	1489	11	8.9	0.211	0.0054	ambient_acidification_on_warming_OWA
GO:0048869	cellular developmental process	276	3	1.65	0.224	0.0174	ambient_acidification_on_warming_OWA